PCCP

PAPER

View Article Online
View Journal | View Issue

Cite this: *Phys. Chem. Chem. Phys.*, 2020, **22**, 18622

C–H activation of light alkanes on MXenes predicted by hydrogen affinity†

Kaifeng Niu,[ab] Lifeng Chi,*[b] Johanna Rosen[a] and Jonas Björk*[a]

C–H activation of light alkanes is one of the most important reactions for a plethora of applications but requires catalysts to operate at feasible conditions. MXenes, a new group of two-dimensional materials, have shown great promise as heterogeneous catalysts for several applications. However, the catalytic activity of MXenes depends on the type and distribution of termination groups. Theoretically, it is desired to search for a relation between the catalytic activity and the termination configuration by employing a simple descriptor in order to avoid tedious activation energy calculations. Here, we show that MXenes are promising for splitting C–H bonds of light alkanes. Furthermore, we present how a quantitative descriptor – the hydrogen affinity – can be used to characterize the termination configuration of Ti_2CT_z (T = O, OH) MXenes, as well as the catalytic activity towards dehydrogenation reactions, using propane as model system. First-principles calculations reveal that the hydrogen affinity can be considered as an intrinsic property of O and OH terminated Ti_2C MXenes, in which the mean hydrogen affinity for the terminated Ti_2C MXenes is linearly correlated to the statistical average of their OH fraction. In addition, the C–H activation energies exhibit a strong scaling relationship to the hydrogen affinity. This quantity can therefore yield quick predictions of catalytic activity of terminated Ti_2C MXenes towards C–H activations, and even predict their chemical selectivity toward scissoring different C–H bonds. We believe that the hydrogen affinity will accelerate the discovery of further applications of the broad family of MXenes in heterogeneous catalysis.

Received 6th May 2020,
Accepted 24th July 2020

DOI: 10.1039/d0cp02471f

rsc.li/pccp

1. Introduction

Light alkanes (C_1 to C_6) are the principal components in petroleum, natural gas and have been widely used as building blocks for the synthesis of plastics, medicines and chemical components.[1–3] For instance, the production of olefins *via* direct C–H activations of light alkanes has been considered as a profitable strategy to satisfy the fast growing demand of olefins in the past several decades.[4] Furthermore, it has been long desired to achieve further reactions, *e.g.* polymerization and cyclodehydrogenation, *via* direct C–H activations of light hydrocarbons.[5,6] Due to the chemical stability of C–H bonds, however, such activations not only require high energy input, but also depend on catalysts with high efficiency.[7] Various strategies have been developed to activate C–H bonds under mild conditions by employing noble metals such as Pt, Pd and Ru.[8–10] Nevertheless, the practical challenge remains in the poor chemoselectivity of C–H activations. Such drawback leads both to low yield and a rapid deactivation due to quenching of active sites by side-products. Conventionally, the efficiency of C–H activations can be increased by applying geometric confinements, *e.g.* reconstructed metal surfaces with grooves, or alloying catalysts with a different metal to create discrete active sites.[11,12] For example, alloyed Pt–Sn catalysts have been widely used for achieving the selective dehydrogenations of propane with high efficiency, in which the over-dehydrogenation process would be effectively prevented due to the presence of Sn atoms.[13–15] Despite this, C–H activations still suffer from obstacles such as high cost and fast deactivation, which can be ascribed to the difficulty in generating catalysts with desired active sites.[16]

Alternatively, two-dimensional (2D) materials, including metal–organic frameworks and metal anchored CN monolayers, have been demonstrated to possess high activity as heterogeneous catalysts due to low-coordinated and uniformly-distributed active sites.[17,18] In particular, MXenes, a bourgeoning class of 2D materials,[19] are of considerable interests in many aspects

[a] *Department of Physics, Chemistry and Biology, IFM, Linköping University, 581 83 Linköping, Sweden. E-mail: jonas.bjork@liu.se*
[b] *Institute of Functional Nano & Soft Materials (FUNSOM) and Jiangsu Key Laboratory for Carbon-Based Functional Materials & Devices, Soochow University, Suzhou 215123, P. R. China. E-mail: chilf@suda.edu.cn*

† Electronic supplementary information (ESI) available: Details of reaction energies and energy barriers of C–H activations on $Ti_2CO_{2-x}(OH)_z$ MXenes. The catalytic origin of the C–H activations at different sites. The reaction pathways for the re-generation of the O active site. The detailed definition of hydrogen affinity. The influence of the H adsorption site on the hydrogen affinity. The distribution of hydrogen affinity with respect to the termination composition on the both sides of MXenes. The correlations between the hydrogen affinity and the reaction energy of C–H activations. See DOI: 10.1039/d0cp02471f

including energy storage, nanoelectronics and catalysis owing to high surface area, tunable electronic structure and good thermal stability.[20,21] MXenes, originated from so called MAX phases,[22] are of the general formula $M_{n+1}X_nT_z$, where M is a transition metal, X is C and/or N, n equals 1–3, and T represents surface termination groups. Previous studies have shown that O terminated MXenes not only exhibit significant properties but also serve as the support surface in anchoring single-atom active sites.[23,24] For instance, the 2D molybdenum MXene (Mo_2CT_2, T = O, OH and F) exhibit a distinguished catalytic activity towards hydrogen evolution reaction (HER) with an initial overpotential of 283 mV.[25] Theoretical calculations have shown that such high activity can be ascribed to O terminal groups on the MXene serving as active sites. However, the catalytic activity of MXenes are profoundly influenced by the termination group distribution.[21] Gao *et al.* have theoretically predicted that the catalytic activity of the terminated MXenes (V_2C, Ti_2C and Ti_3C_2 *etc.*) towards HER can be tuned by achieving different stoichiometric ratios of O and OH terminal groups.[26] Such tunable terminations of MXenes can be achieved by changing the preparation and/or post processing method.[27] Moreover, O-containing groups are demonstrated to be active sites for dehydrogenations on MAX phase catalysts.[28] Recently, Liu and co-works have experimentally achieved the dehydrogenation of ethylbenzene on the fully O terminated Ti_3C_2 MXene, in which the reactivity of the Ti_3C_2 MXene is much higher than that of graphene and nanodiamond.[29] Hence, fully O terminated MXenes are promising as catalysts for dehydrogenations of light alkanes. Furthermore, as OH terminations are a natural consequence of dehydrogenation, their influence is inevitable for such reaction protocols. Therefore, the influence of OH termination on the catalytic activity for MXenes still need to be stressed.

Mechanistically, the C–H activation on an oxygen-promoted catalyst occurs *via* either the catalysts-stabilized or the radical-like pathway.[30] In the first, the dissociated C radicals are stabilized by chemisorption on the catalyst surface, resulting in the co-adsorption of the dissociated H atoms and C radicals (H(ad) + C_nH_{2n+1}(ad)). In the second, however, the radical-like intermediate is stabilized by the formation of OH bond instead of the interactions between the C atom in the radical and the active site, leading to the final state of the reaction as H(ad) + C_nH_{2n+1}(g).[31] As a consequence, the transition state (**TS**) energies for various pathways are distinctively different.[32] The **TS** energy is often characterized by the scaling relationship of chemical reactions – the Brønsted–Evans–Polanyi (BEP) relation – in which the energy of transition state is proportional to the corresponding reaction energy.[33] Such linear relationship has been widely applied to heterogeneous catalysis on transition metals as well as their oxides.[34,35] In addition, Viñes and co-workers have extended the universality of the BEP relation to metal carbides surfaces by using the O_2 dissociation as the model reaction.[36] However, it is debatable to what extent the BEP relation can be used to generalize a particular reaction, and it has been suggested that a distinction should be made by differentiating pristine surfaces from defect sites.[37] Alternatively, previous studies have shown that the activity of the metal oxides is closely related to the functionalization groups. For example, Kostestkyy and co-workers have proposed that the existence of the OH groups would decrease the activity of the metal oxides towards alcohol dehydration.[38] In addition, the hydrogen binding energy has been introduced as a descriptor for unravelling the relationship between the structure and activity of the metal oxide catalysts. For example, a volcano relationship can be observed between activity and dissociated H_2 binding energy of γ-Al_2O_3, while a linear correlation has been established on a range of metal oxides.[39,40] Furthermore, hydrogen affinity (E_H) has been considered as an effective quantitative descriptor for radical-like dehydrogenation of small hydrocarbons.[32,41] For instance, Nørskov and co-workers have proposed a universal linear scaling relation for C–H activation of methane on O promoted transition metal catalysts.[41]

As one of the most widely studied MXenes, Ti_2C with different terminations have shown potential in various catalytic applications.[42] However, the scaling relation between the termination groups and the catalytic activity is still far from understood. Herein, we present the catalytic performance of fully terminated Ti_2C MXenes with various ratios of O and OH groups, $Ti_2CO_{2-z}(OH)_z$ ($0 \leq z \leq 2$), towards the dehydrogenations of propane (C_3H_8), obtained by first-principles calculations. The dehydrogenation of propane may proceed on either the terminal methyl group (–CH_3) or the middle methylene bridge (–CH_2–). It is found that fully O terminated Ti_2C MXenes (Ti_2CO_2) exhibit a good catalytic activity in which the activation energies at the methyl group and the methylene bridge are 2.01 eV and 1.59 eV, respectively. Furthermore, the catalytic activity is significantly influenced by the distribution of termination groups. Further investigations indicate that the catalytic activity of the $Ti_2CO_{2-z}(OH)_z$ ($0 \leq z \leq 2$) MXenes towards C–H activations at both –CH_3 and –CH_2– sites can be described by the BEP relation, in which linear correlations are observed between the activation energies and the corresponding reaction energy. In addition, we show that the hydrogen affinity can be used as a quantitative descriptor for not only probing the termination groups configurations of $Ti_2CO_{2-z}(OH)_z$ MXenes, but also for predicting the catalytic activity and selectivity of the MXene towards the C–H activation. The C–H activation energy of $Ti_2CO_{2-z}(OH)_z$ MXene depends linearly on the corresponding hydrogen affinity, in which the highest activity is achieved on the MXenes with the lowest hydrogen affinity.

2. Methods

The density functional theory (DFT) calculations were performed using Vienna Ab initio Simulation Package (VASP) together with Atomic Simulation Environment (ASE).[43,44] The electron–ion interactions were described by projector augmented wave (PAW) potentials.[45] The exchange–correlation interactions were treated by van der Waals density functional (vdWDF) in the version of rev-vdWDF2 developed by Hamada.[46,47] The cutoff energy for the plane wave basis was set to 400 eV. The periodic image interactions were avoided by employing a vacuum layer of 20 Å.

The transition states search for C–H activations was first calculated with Climbing Image Nudge Elastic Band (CI-NEB), in which 10 images were inserted between initial and final states.[48,49] The central images were then used as the input of the Dimer calculations to obtain accurate transition states.[50] The structure of all local minima and saddle points were optimized until the residual forces were below 0.02 eV $Å^{-1}$. The $p(4 \times 4)$ Ti_2C MXene supercells with O and OH terminal groups were employed as the catalysts, in which the dehydrogenations and the calculations for hydrogen affinity were performed on the top side of MXenes, while the bottom side remained unchanged. The lattice parameter for O terminated Ti_2C MXenes (Ti_2CO_2) was optimized to 3.018 Å. The Brillouin zone of the reciprocal lattice was modeled by gamma-centered Monkhorst–Pack scheme, in which the Γ point and $4 \times 4 \times 1$ grid were adopted for all calculations.[51]

3. Results and discussion

To explore the pathway of propane dehydrogenation, we choose fully O terminated Ti_2C MXenes (Ti_2CO_2) as first model system. Herein, the reactions are considered to take place on the one side of the terminated Ti_2C MXenes, which is defined as the top side. As shown in Fig. 1, the dehydrogenation of the propane on the Ti_2CO_2 MXene consists of two elementary steps, the C–H activation and the drift of the abstracted H atom. First, the intact propane molecule physisorbs on the top side of the Ti_2CO_2 (**IS**). There are then two possible ways the reaction can be initiated: dehydrogenation on the terminal methyl group ($–CH_3$, blue curve) and dehydrogenation on the methylene group ($–CH_2–$, red curve). The C–H activations at both methyl and methylene groups exhibit a radical-like pathway, in which the dehydrogenated radical (C_3H_7) at the transition state (**TS1**) is stabilized by the formation of the OH group (**TS1** in Fig. 1).[41] At **TS1**, the C–H bond lengths are elongated to 2.36 Å and 2.14 Å, at the methyl and methylene group, respectively. The activation energy of the respective C–H activations is defined as

$$E_a = E_{TS1} - E_{IS}, \quad (1)$$

where E_{TS1} and E_{IS} are the total energies of **TS1** and **IS**, respectively. Despite the similarity of reaction pathways for activating C–H bonds, the Ti_2CO_2 exhibits different catalytic activities towards C–H activations at various hydrocarbon groups, in which the C–H bond scission at the $–CH_2–$ group is more energetically favorable with an activation energy (E_a) of 1.59 eV while the activation energy is 2.01 eV at the $–CH_3$ site. Such barrier indicates that the O-terminated MXene exhibits comparable activity towards C–H activations with transition metal catalysts (Pt–Sn alloy).[12] Passing through **TS1**, the dehydrogenated radical and the dissociated H atom co-adsorb at one O atom of the Ti_2CO_2 (**IM**). (We also considered the adsorption of the proxyl radical chemisorbed to the metal site which, however, relaxes into the preferred adsorption to the O atom.) Electronic structure analysis shows that the C–O bonds are formed at the transition complexes, in which electrons are donated from C atoms to the O active sites. In addition, the chemoselectivity of the Ti_2CO_2 towards different C sites of the propane can be ascribed to the stability of the transition complexes. The transition complex of the CH_2 site exhibits stronger interaction with the Ti_2CO_2 catalyst, leading to a lower activation

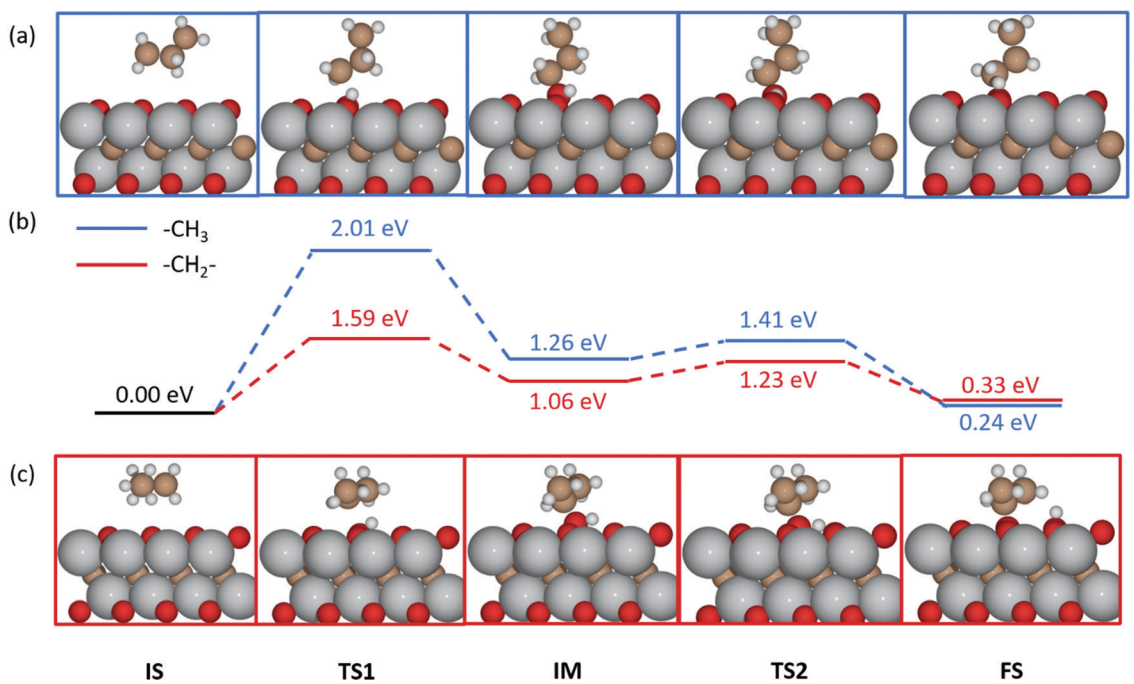

Fig. 1 The reaction pathways for dehydrogenation of (a) the $–CH_3$ and (c) $–CH_2–$ group of propane on the top side of the O terminated Ti_2C MXene (Ti_2CO_2), with (b) the corresponding energy profiles. The blue and red curve represent the energy profiles of the C–H activation at the $–CH_3$ group and the $–CH_2–$ group, respectively. The C, Ti, O and H atoms are represented by brown, silver, red and white circles, respectively.

energy (Fig. S1, ESI†). Subsequently, the dissociated H atom would diffuse to the adjacent O atom with barriers of 0.15 eV and 0.17 eV for $-CH_3$ and $-CH_2-$ site, respectively (**TS2**), which agrees to the previous result on $Ti_3C_2O_2$.[29] Following the dehydrogenation of the $-CH_2-$ site, the resulting 2-proxyl radical, adsorbed on the surface, may either undergo a second C–H activation of the same C atom or of one of the terminal $-CH_3$ sites resulting in propylene. Our calculations show that the former reaction has an activation energy of 2.00 eV, while it is just 1.35 eV for the latter. *i.e.* Ti_2CO_2 exhibits a strong selectivity towards the synthesis of propylene (Fig. S2, ESI†). Notably, the first dehydrogenation step, with a barrier of 1.59 eV, is the rate-limiting step for the overall propylene synthesis. Such reaction pathway with relatively low activation energy shows that the O terminated Ti_2C MXenes are promising catalysts in achieving high-efficiency C–H activations. However, post synthesis processing is required to generate the fully O terminated Ti_2C MXenes,[52] and the termination groups distribution is highly dependent on the etching methods.[53] Furthermore, as dehydrogenation reactions proceed, an initially fully O terminated MXene will unavoidably incorporate OH terminations. Therefore, a systematic investigation on the catalytic activities of the Ti_2C MXenes with various termination groups is needed.

Experimentally, the most common termination groups for MXenes synthesized by HF etching from MAX phases are O, OH and F groups, in which the O termination groups are presumed to be active sites for C–H activations.[53] However, the co-existence of the O and OH terminations is inevitable as the dehydrogenations proceed. Therefore, the regeneration of the O active site from OH groups plays a crucial role in the catalytic performance. Different pathways for removing H atoms were considered, as well as the desorption of H_2O (Fig. S3, ESI†). The energetically most favored pathway includes the conversion of two adjacent OH groups into H_2O and the concomitant associative desorption of H_2, with an effective barrier of 1.90 eV and desorption energy of 0.34 eV. The H_2O may also desorb as an intact molecule, but the overall desorption energy of such a process is 2.09 eV, *i.e.* less likely than the H_2 desorption. The results agree to experimental observations in which OH can be converted into O terminations by heating or an Ar^+ beam.[54,55] However, we cannot exclude the possibility of H_2O desorption, which could be of importance to consider when rejuvenating the catalytic properties of the MXene surface for example by heating.

The co-existence of the O and OH groups on Ti_2C MXenes is commonly observed, and the relative fraction between O and OH groups is naturally the most sensitive characteristics of the MXene termination group configuration during C–H activation. Therefore, we focus on carefully studying how the OH fraction influences the reactivity. We constructed $Ti_2CO_{2-z}(OH)_z$ MXenes and selected 24 surfaces with different terminal group distribution and/or stoichiometry to study the catalytic activity towards C–H activations. In the field of heterogeneous catalysis, the trend of chemical reactions are often quantitatively characterized by the BEP relation, which has been considered as a useful tool to predict the kinetic behavior of a chemical reaction based on thermodynamic data.[36] In the context of C–H activations, the change of the enthalpy can be directly denoted by the reaction energy, the energy difference between the final and initial states. Considering that the C–H scission process (**IS** to **IM** in Fig. 1) is the rate-limiting step in the propane dehydrogenation, the corresponding reaction energy is therefore defined as:

$$E = E_{\mathbf{IM}} - E_{\mathbf{IS}}, \quad (2)$$

where $E_{\mathbf{IM}}$ and $E_{\mathbf{IS}}$ are the total energies of **IM** and **IS**, respectively. Such reaction energies are calculated to correlate the catalytic activity of MXenes with different termination groups.[29] Fig. 2 shows the linear correlation between the reaction and activation energies, in which the C–H activation at the $-CH_3$

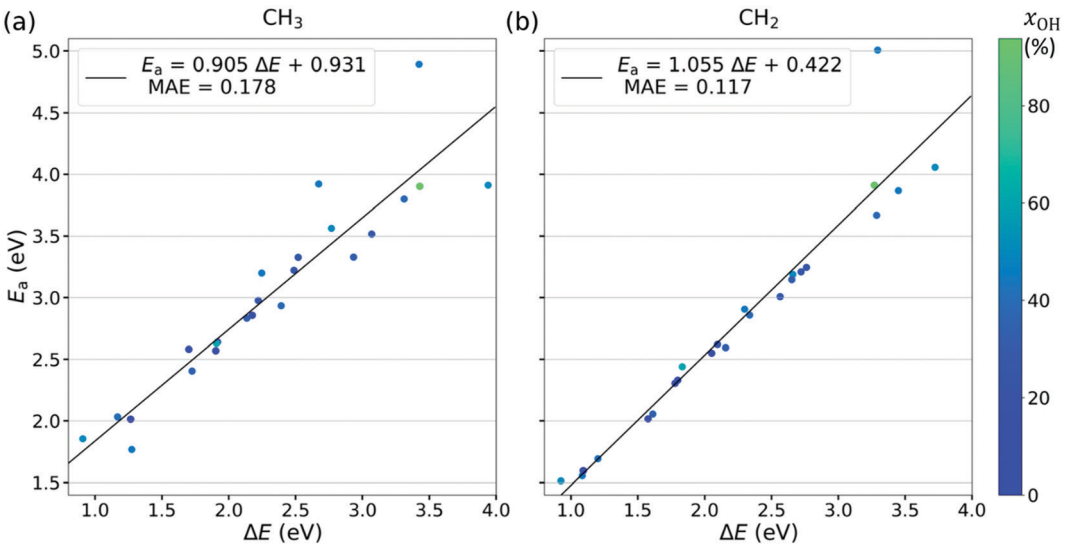

Fig. 2 The Brønsted–Evans–Polanyi (BEP) correlations for dehydrogenations at the (a) terminal methyl group ($-CH_3$) and (b) methylene bridge ($-CH_2-$) of propane. The C–H activation energies (E_a) increase as the reaction energies (E) increase. The color bar from blue to green corresponds to the fraction of OH groups in the $Ti_2CO_{2-z}(OH)_z$ MXenes from fully O terminated Ti_2C (0%) to fully OH terminated Ti_2C (100%).

and –CH_2– groups can be lumped into separate BEP relations. As seen, the activation energy exhibits a strong proportional correlation with the corresponding reaction energy, suggesting that the catalytic activity decreases as the energy of **IM** increases with respect to that of **IS**. These results agree well with elementary reactions at metal surfaces.[33] Despite that the BEP relation has been proved applicable for C–H activations on the OH and O terminated Ti_2C MXenes, the prediction and characterization of the activity is still limited by the difficulty in optimizing the initial and final states for a reaction. In addition, outliers in the BEP relation are observed at the surface with the highest OH ratio on the top side. Such outliers can be ascribed to a steric hindrance that increases the energy of the transition states. Thus, it is useful to examine the implications of accurately predicting C–H activation energies with an intuitive and more efficient descriptor.[41]

The fraction of OH groups (x_{OH}), on the other hand, as one of the intrinsic properties of the terminated MXenes, can be directly accessed from post analysis after the synthesis. Here, the x_{OH} is defined by the ratio of OH groups to all termination groups:

$$x_{OH} = N_{OH}/(N_{OH} + N_O), \quad (3)$$

in which the N_{OH} and N_O denote the number of OH groups and O groups in the MXene, respectively. Previous theoretical studies have shown that it is possible to use the x_{OH} to characterize the catalytic activity of the MXenes, in which the low x_{OH} would effectively promote the catalytic activity.[25,56] Nevertheless, DFT calculations show that such a simple descriptor is not sufficient to quantitatively describe the activity of Ti_2CT_z MXenes. The reaction energies of C–H activations at the –CH_3 and –CH_2– groups are significantly influenced by the fraction of the OH group in $Ti_2CO_{2-z}(OH)_z$ MXenes, in which the barriers for the C–H bond scission are strongly varied as the fraction of OH changes (see Table S1 in the ESI†). Nevertheless, there is no obvious trend between the catalytic activity of $Ti_2CO_{2-z}(OH)_z$ MXenes and this quantity. A high fraction of OH groups does not always lead to poor catalytic activity for C–H splitting and a low fraction of OH does not always result in good activity (Table S1, ESI†). Moreover, such simple model fails to distinguish the activity of $Ti_2CO_{2-z}(OH)_z$ MXenes with the same amount of OH termination groups but different configurations. For example, the reaction energies for the dehydrogenation of the methyl group on the $Ti_2CO_{2-z}(OH)_z$ MXenes with 50% of OH groups are found within a range of 3 eV, suggesting that the fraction of OH is not the main determining factor of the catalytic activities. Instead, we found that the hydrogen affinity is a more suitable quantity to connect the configuration and reactivity of a MXene surface.

The hydrogen affinity (E_H) represents the ability of an oxide species to abstract an H atom, defined as

$$E_H = E(M_mO_xH_{y+1}) - E(M_mO_xH_y) + \frac{1}{4}E(O_2) - \frac{1}{2}E(H_2O), \quad (4)$$

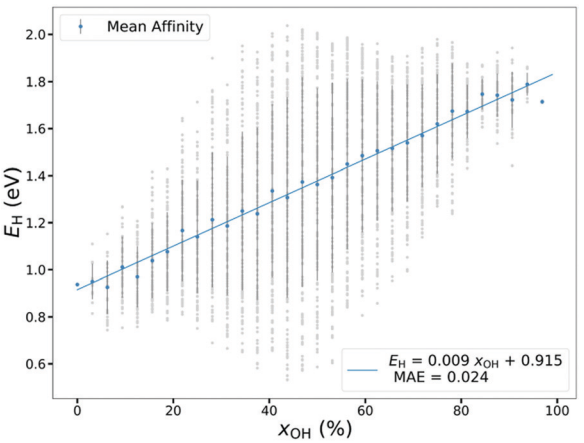

Fig. 3 The correlation between the hydrogen affinity (E_H) and the fraction of OH groups of $Ti_2CO_{2-z}(OH)_z$ MXenes (x_{OH}). Grey points represent the E_H values for each $Ti_2CO_{2-z}(OH)_z$. Blue dots with vertical lines represent the mean E_H for each fraction of OH groups with the standard deviation. The blue line is the linear regression of the mean E_H with respect to the fraction of OH groups.

where the $E(M_mO_xH_{y+1})$, $E(M_mO_xH_y)$, $E(H_2O)$ and $E(O_2)$ are referred to the potential energy of the catalyst with an extra H atom, the original catalyst, a water molecule and an oxygen molecule, respectively (detailed definition is shown in ESI†).[41,57] Such descriptor has been successfully utilized to predict the catalytic activities of O promoted catalysts towards the C–H and C–O activations, in which the catalytic activity decreases as the E_H increases.[57,58] Based on the definition, the E_H of $Ti_2CO_{2-z}(OH)_z$ MXenes can be influenced by several factors: the overall fraction of OH groups (x_{OH}), the configuration of the termination groups and the adsorption site of the H atom. However, DFT calculations show that the difference between E_H values between different sites for a $Ti_2CO_{2-z}(OH)_z$ MXene with a specific termination configuration is negligible (Table S2, ESI†). Therefore, subsequent investigations focus on the correlation between the E_H and the distribution of the termination groups.

The termination configuration of MXenes are determined by three dimensions: the fraction of OH groups on the top ($x_{OH\text{-}top}$), the fraction of OH groups on the bottom ($x_{OH\text{-}bottom}$) and the distributions of the OH groups on both sides of the MXenes. In our case, the top side of the MXene is defined as the surface where the H adsorption and reactions take place. The definition of $x_{OH\text{-}top}$ and $x_{OH\text{-}bottom}$ follows eqn (3), by only considering the number of termination groups on each side of the MXene. Subsequently, the hydrogen affinity of $Ti_2CO_{2-z}(OH)_z$ MXenes with all possible $x_{OH\text{-}top}$ and $x_{OH\text{-}bottom}$ combinations are investigated. For each combination, 10 structures with different termination group distribution were considered, resulting in a number of 2762 different $Ti_2CO_{2-z}(OH)_z$ MXenes. Fig. 3 shows the hydrogen affinity as a function of the average OH-fraction on both top and bottom of the MXene. The formation of the OH group on all terminated Ti_2C MXenes are endothermic ($E_H > 0$ eV), indicating that O terminal groups are more stable than OH terminal groups.[53] Statistically, the mean E_H for $Ti_2CO_{2-z}(OH)_z$ MXenes exhibits a good linear relation with the fraction of

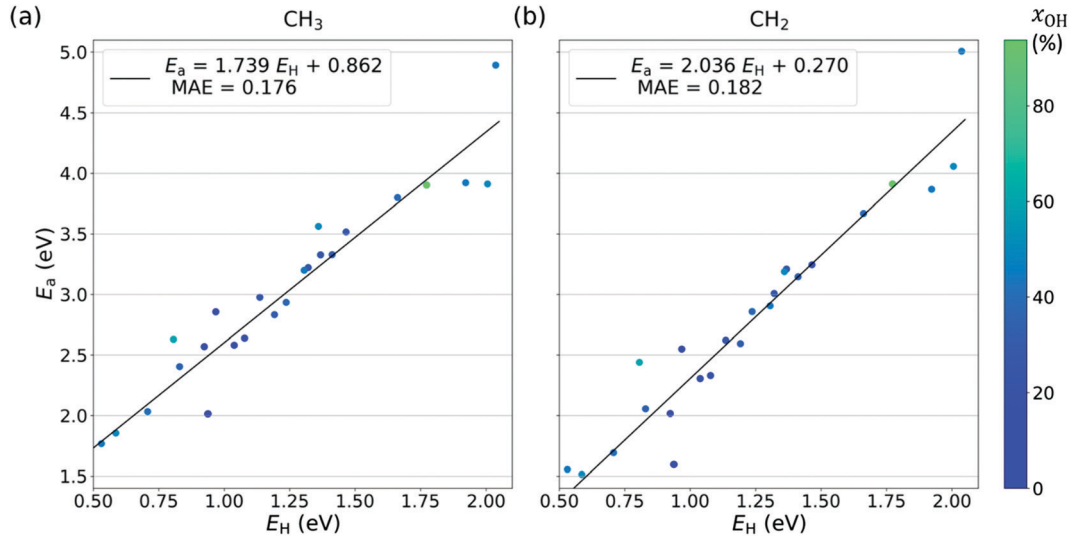

Fig. 4 The scaling relationships between the activation energies (E_a) and the hydrogen affinities (E_H) for C–H activations at (a) $-CH_3$ and (b) $-CH_2-$ group in the propane that proceed on the $Ti_2CO_{2-z}(OH)_z$ MXenes. The color map represents the overall fraction of OH groups of the MXenes.

OH groups. Such generalized relation indicates that the E_H can be used to characterize the termination configuration of the terminated Ti_2C MXenes. Of importance, the E_H is strongly influenced by the distribution of termination groups. As seen in Fig. 3, the standard deviation for the hydrogen affinity at each overall OH fraction is relatively large (grey lines). For instance, the range of E_H is larger than 1.50 eV for $Ti_2CO(OH)$ MXenes (the fraction of OH is 50%). Such significant deviation suggests the hydrogen affinity is determined by not only the overall fraction of OH groups but also the termination group distribution.

Further analysis shows that the hydrogen affinity can be considered as an intrinsic property of the termination configuration of Ti_2C MXenes. Note that the smallest E_H (0.53 eV) and the largest E_H (2.04 eV) can be found at the $Ti_2CO_{2-z}(OH)_z$ MXene with the same fraction of OH groups (x_{OH} = 43.75%) with different configurations of termination groups, suggesting that the hydrogen affinity is determined by the termination groups distribution. Specifically, the fraction of OH groups on the top ($x_{OH\text{-}top}$) plays an important role in determining the hydrogen affinity. For instance, the MXene with the lowest $x_{OH\text{-}top}$ and the highest $x_{OH\text{-}bottom}$ combination possesses the smallest E_H, while the $Ti_2CO_{2-z}(OH)_z$ with highest $x_{OH\text{-}top}$ and lowest $x_{OH\text{-}bottom}$ exhibits the largest hydrogen affinity (detailed relation between E_H and termination groups distribution is extracted in Fig. S5, ESI†). Such result indicates that the hydrogen affinity can be used for distinguishing the catalytic activities of MXenes with the same amount of OH groups.

Of importance, the hydrogen affinity can not only represent the termination configuration of $Ti_2CO_{2-z}(OH)_z$ MXenes but also characterize the catalytic activity of the active sites on the top side. First of all, the reaction energies for C–H activations of both the $-CH_3$ and $-CH_2-$ groups of propane on $Ti_2CO_{2-z}(OH)_z$ MXenes have linear relationships with their corresponding hydrogen affinities (Fig. S6, ESI†). Based on the BEP relation, the activation energies depend linearly on the reaction energies (*vide supra*). Therefore, the activation energies would increase as the hydrogen affinity increases. As expected, the catalytic activity of $Ti_2CO_{2-z}(OH)_z$ MXenes towards C–H activations increases as the hydrogen affinity approaches to 0 eV for both the $-CH_3$ and $-CH_2-$ groups (Fig. 4). Such trends agree well with previous studies, where the catalytic activity towards oxidative dehydrogenation of cyclohexane on Co_3O_4 nanoparticles can be promoted by reducing the hydrogen affinity of active sites.[58] In addition, the highest activation energies for both C–H activations are obtained on the MXene possessing the highest E_H (2.04 eV) with a stoichiometry of O and OH groups as $Ti_2CO_{1.125}(OH)_{0.875}$. The underlying mechanism of the poor activity can be ascribed to limited number active sites on the top side to proceed the C–H activations ($x_{OH\text{-}top}$ = 87.5% from Fig. S6, ESI†). Therefore, the catalytic activity of the MXenes with the same fraction of OH groups but different distribution can be significantly different. Notably, both the reaction and activation energies are described by a linear relationship with respect to the hydrogen affinity. Thus, simply by calculating the hydrogen affinity of a MXene it is possible to quantitatively assess its activity towards dehydrogenation, within an error margin.

From the trends in Fig. 4, it is revealed that the MXenes with low hydrogen affinity (E_H < 1.0 eV) exhibit higher activity towards activating the CH_2 group than that of CH_3 group. The difference in activation energies (>0.20 eV) is even larger than that of noble metal catalysts (*e.g.* Pt/Sn alloy).[12] Such distinction in the activity implies that O and OH terminated MXenes have a great potential to be good catalysts for the high-selective catalysts for further functionalization of light hydrocarbons.

4. Conclusions

In conclusion, C–H activations of propane on $Ti_2CO_{2-z}(OH)_z$ MXenes have been investigated based on DFT calculations. The

Ti_2CO_2 MXene exhibits high catalytic activity towards the C–H activations and the co-existence of multiple termination groups is one of the most vital factors for predicting the catalytic activity. In particular, we propose the hydrogen affinity (E_H) as a quantitative descriptor both for characterizing the termination configuration and probing the catalytic activity and selectivity of the $Ti_2CO_{2-z}(OH)_z$ MXenes, which is not possible by models based purely on thermodynamics or chemical composition. The mean affinity of the overall OH fraction increases as the OH fraction approaches 100%, indicating that Ti_2C MXenes with fewer OH terminations are more likely to abstract an H atom from the reactant. Further analysis shows that the catalytic activity is linearly correlated with the hydrogen affinity, in which highly active MXenes possess low hydrogen affinity. It is anticipated that the hydrogen affinity can serve as a theoretical descriptor for efficient evaluation of catalytic activities of terminated Ti_2C MXenes and pave the way for the rational design of MXenes based catalysts in general.

Conflicts of interest

The authors declare no competing financial interest.

Acknowledgements

We acknowledge the Collaborative Innovation Centre of Suzhou Nano Science & Technology, the Priority Academic Program Development of Jiangsu Higher Education Institutions (PAPD), and the 111 Project. This work was supported by the Swedish Research Council and the Swedish Government Strategic Research Area in Materials Science on Functional Materials at Linköping University (Faculty Grant SFO-Mat-LiU No. 2009 00971), the National Natural Science Foundation of China (NSFC, Grant No. 21790053, and 51821002) and the Major State Basic Research Development Program of China (2017YFA0205000). Computational resources were allocated at the National Supercomputer Centre, Sweden, allocated by SNIC. J. R. acknowledges funding from the Knut and Alice Wallenberg (KAW) Foundation for a Fellowship grant, and from the Swedish Foundation for Strategic Research (SSF) for program funding (EM16-0004).

References

1 F. D. Mango, The Light Hydrocarbons in Petroleum: A Critical Review, *Org. Geoclwm.*, 1996, **26**, 417–440.
2 L. Nykanen and K. Honkala, Selectivity in Propene Dehydrogenation on Pt and Pt_3Sn Surfaces from First Principles, *ACS Catal.*, 2013, **3**, 3026–3030.
3 K. Sun, A. Chen, M. Liu, H. Zhang, R. Duan, P. Ji, L. Li, Q. Li, C. Li, D. Zhong, K. Mullen and L. Chi, Surface-Assisted Alkane Polymerization: Investigation on Structure-Reactivity Relationship, *J. Am. Chem. Soc.*, 2018, **140**, 4820–4825.
4 Z. Nawaz, Light Alkane Dehydrogenation to Light Olefin Technologies: a Comprehensive Review, *Rev. Chem. Eng.*, 2015, **31**, 413–436.
5 L. Yin and J. Liebscher, Carbon–carbon Coupling Reactions Catalyzed by Heterogeneous Palladium Catalysts, *Chem. Rev.*, 2007, **107**, 133–173.
6 D. H. Wang, T. S. Mei and J. Q. Yu, Versatile Pd(II)-catalyzed C–H Activation/Aryl–aryl Coupling of Benzoic and Phenyl Acetic Acids, *J. Am. Chem. Soc.*, 2008, **130**, 17676–17677.
7 Q. Sun, C. Zhang, H. Kong, Q. Tan and W. Xu, On-surface Aryl–aryl Coupling via Selective C–H Activation, *Chem. Commun.*, 2014, **50**, 11825–11828.
8 I. M. Ciobica, F. Frechard, R. A. van Santen, A. W. Kleyn and J. Hafner, A DFT Study of Transition States for C–H Activation on the Ru(0001) Surface, *J. Phys. Chem. B*, 2000, **104**, 3364–3369.
9 M. S. Liao, C. T. Au and C. F. Ng, Methane Dissociation on Ni, Pd, Pt and Cu Metal(111) Surfaces – A Theoretical Comparative Study, *Chem. Phys. Lett.*, 1997, **272**, 445–452.
10 M. A. Petersen, S. J. Jenkins and D. A. King, Theory of Methane Dehydrogenation on Pt{110} (1×2). Part I: Chemisorption of CH_x (x = 0–3), *J. Phys. Chem. B*, 2004, **108**, 5909–5919.
11 D. Zhong, J. H. Franke, S. K. Podiyanachari, T. Blomker, H. Zhang, G. Kehr, G. Erker, H. Fuchs and L. Chi, Linear Alkane Polymerization on a Gold, *Surf. Sci.*, 2011, **334**, 213–216.
12 M. L. Yang, Y. A. Zhu, X. G. Zhou, Z. J. Sui and D. Chen, First-Principles Calculations of Propane Dehydrogenation over PtSn Catalysts, *ACS Catal.*, 2012, **2**, 1247–1258.
13 O. A. Barias, A. Holmen and E. A. Blekkan, Propane Dehydrogenation over Supported Pt and Pt–Sn Catalysts: Catalyst Preparation, Characterization, and Activity Measurements, *J. Catal.*, 1996, **158**, 1–12.
14 A. Valcarcel, J. M. Ricart, A. Clotet, F. Illas, A. Markovits and C. Minot, Theoretical Study of Dehydrogenation and Isomerisation Reactions of Propylene on Pt(111), *J. Catal.*, 2006, **241**, 115–122.
15 H. B. Zhu, D. H. Anjum, Q. X. Wang, E. Abou-Hamad, L. Emsley, H. L. Dong, P. Laveille, L. D. Li, A. K. Samal and J. M. Basset, Sn Surface-enriched Pt–Sn Bimetallic Nanoparticles as a Selective and Stable Catalyst for Propane Dehydrogenation, *J. Catal.*, 2014, **320**, 52–62.
16 S. Vajda, M. J. Pellin, J. P. Greeley, C. L. Marshall, L. A. Curtiss, G. A. Ballentine, J. W. Elam, S. Catillon-Mucherie, P. C. Redfern, F. Mehmood and P. Zapol, Subnanometre Platinum Clusters as Highly Active and Selective Catalysts for the Oxidative Dehydrogenation of Propane, *Nat. Mater.*, 2009, **8**, 213–216.
17 F. Besenbacher, I. I. Chorkendorff, B. S. Clausen, B. Hammer, A. M. Molenbroek, J. K. Norskov and I. I. Stensgaard, Design of a Surface Alloy Catalyst for Steam Reforming, *Science*, 1998, **279**, 1913–1915.
18 L. Z. Gai, C. T. To and K. S. Chan, Direct Arylation of Aromatic C–H bond Catalyzed by Phthalocyanine, *Tetrahedron Lett.*, 2014, **55**, 6373–6376.
19 M. Naguib, M. Kurtoglu, V. Presser, J. Lu, J. Niu, M. Heon, L. Hultman, Y. Gogotsi and M. W. Barsoum, Two-dimensional Nanocrystals Produced by Exfoliation of Ti_3AlC_2, *Adv. Mater.*, 2011, **23**, 4248–4253.

20 Y. Zhou, K. Luo, X. Zha, Z. Liu, X. Bai, Q. Huang, Z. Guo, C.-T. Lin and S. Du, Electronic and Transport Properties of Ti_2CO_2 MXene Nanoribbons, *J. Phys. Chem. C*, 2016, **120**, 17143–17152.

21 Z. Li and Y. Wu, 2D Early Transition Metal Carbides (MXenes) for Catalysis, *Small*, 2019, 1804736.

22 M. W. Barsoum, The $M_{N+1}AX_N$ Phases: A New Class of Solids: Thermodynamically Stable Nanolaminates, *Prog. Solid State Chem.*, 2000, **28**, 201–281.

23 Z. Guo, J. Zhou, L. Zhu and Z. Sun, MXene: a promising photocatalyst for water splitting, *J. Mater. Chem. A*, 2016, **4**, 11446–11452.

24 Q. Peng, J. Zhou, J. Chen, T. Zhang and Z. Sun, Cu single atoms on Ti_2CO_2 as a highly efficient oxygen reduction catalyst in a proton exchange membrane fuel cell, *J. Mater. Chem. A*, 2019, **7**, 26062–26070.

25 Z. W. Seh, K. D. Fredrickson, B. Anasori, J. Kibsgaard, A. L. Strickler, M. R. Lukatskaya, Y. Gogotsi, T. F. Jaramillo and A. Vojvodic, Two-Dimensional Molybdenum Carbide (MXene) as an Efficient Electrocatalyst for Hydrogen Evolution, *ACS Energy Lett.*, 2016, **1**, 589–594.

26 G. Gao, A. P. O'Mullane and A. Du, 2D MXenes: A New Family of Promising Catalysts for the Hydrogen Evolution Reaction, *ACS Catal.*, 2016, **7**, 494–500.

27 Y. Wen, T. E. Rufford, X. Chen, N. Li, M. Lyu, L. Dai and L. Wang, Nitrogen-doped $Ti_3C_2T_x$ MXene Electrodes for High-performance Supercapacitors, *Nano Energy*, 2017, **38**, 368–376.

28 W. H. K. Ng, E. S. Gnanakumar, E. Batyrev, S. K. Sharma, P. K. Pujari, H. F. Greer, W. Zhou, R. Sakidja, G. Rothenberg, M. W. Barsoum and N. R. Shiju, The Ti_3AlC_2 MAX Phase as an Efficient Catalyst for Oxidative Dehydrogenation of *n*-Butane, *Angew. Chem., Int. Ed.*, 2018, **57**, 1485–1490.

29 J. Diao, M. Hu, Z. Lian, Z. Li, H. Zhang, F. Huang, B. Li, X. Wang, D. S. Su and H. Liu, $Ti_3C_2T_x$ MXene Catalyzed Ethylbenzene Dehydrogenation: Active Sites and Mechanism Exploration from both Experimental and Theoretical Aspects, *ACS Catal.*, 2018, **8**, 10051–10057.

30 G. Kumar, S. L. J. Lau, M. D. Krcha and M. J. Janik, Correlation of Methane Activation and Oxide Catalyst Reducibility and Its Implications for Oxidative Coupling, *ACS Catal.*, 2016, **6**, 1812–1821.

31 Z. J. Zhao, A. Kulkarni, L. Vilella, J. K. Norskov and F. Studt, Theoretical Insights into the Selective Oxidation of Methane to Methanol in Copper-Exchanged Mordenite, *ACS Catal.*, 2016, **6**, 3760–3766.

32 A. A. Latimer, H. Aljama, A. Kakekhani, J. S. Yoo, A. Kulkarni, C. Tsai, M. Garcia-Melchor, F. Abild-Pedersen and J. K. Norskov, Mechanistic Insights into Heterogeneous Methane Activation, *Phys. Chem. Chem. Phys.*, 2017, **19**, 3575–3581.

33 T. Bligaard, J. K. Nørskov, S. Dahl, J. Matthiesen, C. H. Christensen and J. Sehested, The Brønsted–Evans–Polanyi Relation and the Volcano Curve in Heterogeneous Catalysis, *J. Catal.*, 2004, **224**, 206–217.

34 J. Cheng, P. Hu, P. Ellis, S. French, G. Kelly and C. M. Lok, Brønsted-Evans-Polanyi Relation of Multistep Reactions and Volcano Curve in Heterogeneous Catalysis, *J. Phys. Chem. C*, 2008, **112**, 1308–1311.

35 A. Vojvodic, F. Calle-Vallejo, W. Guo, S. Wang, A. Toftelund, F. Studt, J. I. Martinez, J. Shen, I. C. Man, J. Rossmeisl, T. Bligaard, J. K. Noorskov and F. Abild-Pedersen, On the Behavior of Brønsted–Evans–Polanyi relations for Transition Metal Oxides, *J. Chem. Phys.*, 2011, **134**, 244509.

36 F. Viñes, A. Vojvodic, F. Abild-Pedersen and F. Illas, Brønsted–Evans–Polanyi Relationship for Transition Metal Carbide and Transition Metal Oxide Surfaces, *J. Phys. Chem. C*, 2013, **117**, 4168–4171.

37 J. K. Nørskov, T. Bligaard, A. Logadottir, S. Bahn, L. B. Hansen, M. Bollinger, H. Bengaard, B. Hammer, Z. Sljivancanin, M. Mavrikakis, Y. Xu, S. Dahl and C. J. H. Jacobsen, Universality in Heterogeneous Catalysis, *J. Catal.*, 2002, **209**, 275–278.

38 P. Kostestkyy, J. Yu, R. J. Gorte and G. Mpourmpakis, Structure–activity relationships on metal-oxides: alcohol dehydration, *Catal. Sci. Technol.*, 2014, **4**, 3861–3869.

39 P. Deshlahra and E. Iglesia, Methanol Oxidative Dehydrogenation on Oxide Catalysts: Molecular and Dissociative Routes and Hydrogen Addition Energies as Descriptors of Reactivity, *J. Phys. Chem. C*, 2014, **118**, 26115–26129.

40 M. Dixit, P. Kostetskyy and G. Mpourmpakis, Structure–Activity Relationships in Alkane Dehydrogenation on γ-Al_2O_3: Site-Dependent Reactions, *ACS Catal.*, 2018, **8**, 11570–11578.

41 A. A. Latimer, A. R. Kulkarni, H. Aljama, J. H. Montoya, J. S. Yoo, C. Tsai, F. Abild-Pedersen, F. Studt and J. K. Norskov, Understanding Trends in C–H bond Activation in Heterogeneous Catalysis, *Nat. Mater.*, 2017, **16**, 225–229.

42 A. D. Handoko, K. H. Khoo, T. L. Tan, H. M. Jin and Z. W. Seh, Establishing new scaling relations on two-dimensional MXenes for CO_2 electroreduction, *J. Mater. Chem. A*, 2018, **6**, 21885–21890.

43 A. Hjorth Larsen, J. Jorgen Mortensen, J. Blomqvist, I. E. Castelli, R. Christensen, M. Dulak, J. Friis, M. N. Groves, B. Hammer, C. Hargus, E. D. Hermes, P. C. Jennings, P. Bjerre Jensen, J. Kermode, J. R. Kitchin, E. Leonhard Kolsbjerg, J. Kubal, K. Kaasbjerg, S. Lysgaard, J. Bergmann Maronsson, T. Maxson, T. Olsen, L. Pastewka, A. Peterson, C. Rostgaard, J. Schiotz, O. Schutt, M. Strange, K. S. Thygesen, T. Vegge, L. Vilhelmsen, M. Walter, Z. Zeng and K. W. Jacobsen, The Atomic Simulation Environment – a Python Library for Working with Atoms, *J. Phys.: Condens. Mater.*, 2017, **29**, 273002.

44 G. Kresse and J. Furthmuller, Efficient Iterative Schemes for ab-initio Total-energy Calculations Using a Plane-wave Basis Set, *Phys. Rev. B: Condens. Matter Mater. Phys.*, 1996, **54**, 11169–11186.

45 P. E. Blöch, Projector Agumented-wave Method, *Phys. Rev. B: Condens. Matter Mater. Phys.*, 1994, **50**, 17953.

46 M. Dion, H. Rydberg, E. Schroder, D. C. Langreth and B. I. Lundqvist, van der Waals Density Functional for General Geometries, *Phys. Rev. Lett.*, 2004, **92**, 246401.

47 I. Hamada, van der Waals Density Functional Made Accurate, *Phys. Rev. B: Condens. Matter Mater. Phys.*, 2014, **89**, 121103.

48 G. Henkelman and H. Jónsson, Improved Tangent Estimate in the Nudged Elastic Band Method for Finding Minimum Energy Paths and Saddle Points, *J. Chem. Phys.*, 2000, **113**, 9978–9985.

49 G. Henkelman, B. P. Uberuaga and H. Jonsson, A Climbing Image Nudged Elastic Band Method for Finding Saddle Points and Minimum Energy Paths, *J. Chem. Phys.*, 2000, **113**, 9901–9904.

50 G. Henkelman and H. Jonsson, A Dimer Method for Finding Saddle Points on High Dimensional Potential Surfaces using Only First Derivatives. Special Points for Brillouin-Zone Integrations, *J. Chem. Phys.*, 1999, **111**, 7010–7022.

51 H. J. Monkhorst and J. D. Pack, Special Points for Brillouin-Zone Integrations, *Phys. Rev. B: Solid State*, 1976, **13**, 5188–5192.

52 I. Persson, L. A. Naslund, J. Halim, M. W. Barsoum, V. Darakchieva, J. Palisaitis, J. Rosen and P. O. A. Persson, On the Organization and Thermal Behavior of Functional Groups on Ti_3C_2 MXene Surfaces in Vacuum, *2D Mater.*, 2018, **5**, 015002–015011.

53 T. Hu, Z. Li, M. Hu, J. Wang, Q. Hu, Q. Li and X. Wang, Chemical Origin of Termination-Functionalized MXenes: $Ti_3C_2T_2$ as a Case Study., *J. Phys. Chem. C*, 2017, **121**, 19254–19261.

54 O. Mashtalir, M. Naguib, B. Dyatkin, Y. Gogotsi and M. W. Barsoum, Kinetics of Aluminum Extraction from Ti_3AlC_2 in Hydrofluoric Acid, *Mater. Chem. Phys.*, 2013, **139**, 147–152.

55 J. Halim, K. M. Cook, M. Naguib, P. Eklund, Y. Gogotsi, J. Rosen and M. W. Barsoum, X-ray photoelectron spectroscopy of select multi-layered transition metal carbides (MXenes), *Appl. Surf. Sci.*, 2016, **362**, 406–417.

56 Y. Jiang, T. Sun, X. Xie, W. Jiang, J. Li, B. Tian and C. Su, Oxygen Functionalized Ultrathin $Ti_3C_2T_x$ MXene for Enhanced Electrocatalytic Hydrogen Evolution, *ChemSusChem*, 2019, 1368–1373.

57 G. Fu, Z. N. Chen, X. Xu and H. L. Wan, Understanding the Reactivity of the Tetrahedrally Coordinated High-valence d(0) Transition Metal Oxides toward the C–H Bond Activation of Alkanes: A Cluster Model Study, *J. Phys. Chem. A*, 2008, **112**, 717–721.

58 E. C. Tyo, C. R. Yin, M. Di Vece, Q. Qian, G. Kwon, S. Lee, B. Lee, J. E. DeBartolo, S. Seifert, R. E. Winans, R. Si, B. Ricks, S. Goergen, M. Rutter and B. Zugic, M. Oxidative Dehydrogenation of Cyclohexane on Cobalt Oxide (Co_3O_4) Nanoparticles: The Effect of Particle Size on Activity and Selectivity, *ACS Catal.*, 2012, **2**, 2409–2423.